Redox Biology 47 (2021) 102141

Contents lists available at ScienceDirect

Redox Biology

journal homepage: www.elsevier.com/locate/redox

Deacetylation-dependent regulation of PARP1 by SIRT2 dictates ubiquitination of PARP1 in oxidative stress-induced vascular injury

Naijin Zhang [a,b,1], Ying Zhang [a,b,1], Boquan Wu [a], Shaojun Wu [a], Shilong You [a], Saien Lu [a], Jingwei Liu [c,d], Xinyue Huang [a], Jiaqi Xu [a], Liu Cao [c,d,**], Yingxian Sun [a,b,*]

[a] Department of Cardiology, First Hospital of China Medical University, 155 Nanjing North Street, Heping District, 110001, Shenyang, Liaoning, PR China
[b] Institute of Health Sciences, China Medical University, 77 Puhe Road, Shenbei New District, Shenyang, 110001, Liaoning Province, PR China
[c] Key Laboratory of Medical Cell Biology, Ministry of Education, 77 Puhe Road, Shenbei New District, Shenyang, 110001, Liaoning Province, PR China
[d] Institute of School of Basic Medicine, China Medical University, 77 Puhe Road, Shenbei New District, Shenyang, 110001, Liaoning Province, PR China

ARTICLE INFO

Keywords:
SIRT2
WWP2
PARP1
Acetylation
Ubiquitination

ABSTRACT

Poly(ADP-ribose) polymerase 1 (PARP1) has a major regulatory role in cardiovascular disease. However, inhibiting PARP1 activity does not significantly improve clinical outcomes of cardiovascular disease, which suggests that the regulatory mechanism of PARP1 in cardiovascular disease is unclear. Here, we focused on deacetylation regulatory mechanisms of PARP1 and crosstalk of PARP1 post-translational modifications. We uncovered the crucial molecular interactions and protein modifications of deacetylase Sirtuin 2 (SIRT2) and PARP1 in vascular damage. The results showed that SIRT2 was involved in this process and oxidative stress damage factor PARP1 was a novel physiological substrate of SIRT2. SIRT2 interacted with PARP1 at the PARP-A-helical domain and deacetylated the K249 residue of PARP1. Furthermore, SIRT2 promoted ubiquitination of the K249 residue of PARP1 via mobilization of the E3 ubiquitin ligase WW domain-containing protein 2 (WWP2), which led to proteasome-mediated degradation of PARP1. Knockout of SIRT2 in mice and cells increased PARP1 acetylation and decreased PARP1 ubiquitination, which in turn aggravated oxidative stress-induced vascular injury and remodeling. Conversely, overexpression of SIRT2 in mice and cells decreased PARP1 acetylation, increased PARP1 ubiquitination, and relieved oxidative stress-induced vascular injury and remodeling. Overall, this study revealed a previously unrecognized mechanistic link between SIRT2 and PARP1 in the regulation of oxidative stress-induced vascular injury.

1. Introduction

Oxidative stress-induced vascular injury is the primary and critical factor that affects various cardiovascular diseases [1–3]. Consequently, clarification of the responsible molecular mechanisms has become a priority. The oxidative stress injury-related protein poly(ADP-ribose) polymerase 1 (PARP1) is a major factor in cardiovascular disease. Recently, it was reported that PARP1 plays a crucial role in oxidative stress-induced vascular injury that eventually damages various organs [4–8]. Indeed, various stimulating factors aggravate vascular oxidative stress by over-activating PARP1, which leads to vascular damage and cell death [4,5]. Although most studies have focused on the treatment of cardiovascular disease by inhibiting PARP1 activity, there has been no significant improvement of clinical outcomes in cardiovascular disease, which suggests that the regulatory mechanism of PARP1 in cardiovascular disease is unclear.

Expression of PARP1 is tightly controlled at transcriptional levels, but high expression of PARP1 is observed in cardiovascular disease [6–8]. Importantly, enhanced expression of PARP1 is critical during cardiovascular disease. Our previous study revealed that PARP1 as the major factor in oxidative stress-induced cardiovascular injury undergoes ubiquitination by E3 ubiquitin ligase WW domain-containing protein 2 (WWP2) [6,7]. However, lysine deacetylation of non-histone proteins

* Corresponding author. Department of Cardiology, First Hospital of China Medical University, 155 Nanjing North Street, Heping District, 110001, Shenyang, Liaoning, PR China.
** Corresponding author. Key Laboratory of Medical Cell Biology, Ministry of Education, 77 Puhe Road, Shenbei New District, Shenyang, 110001, Liaoning Province, PR China.
E-mail addresses: lcao@cmu.edu.cn (L. Cao), yxsun@cmu.edu.cn (Y. Sun).
[1] These authors contributed equally to this work as first authors.

https://doi.org/10.1016/j.redox.2021.102141
Received 26 August 2021; Received in revised form 12 September 2021; Accepted 16 September 2021
Available online 20 September 2021

Abbreviations

PARP1	poly(ADP-ribose) polymerase 1
SIRT2	Sirtuin 2
ROS	reactive oxygen species
Ang II	angiotensin II
KO	knockout
TG	transgenic
HE	hematoxylin and eosin
HUVECs	human umbilical vein endothelial cells
WWP2	WW domain-containing protein 2
FBS	fetal bovine serum
SD	standard deviation
CHX	cycloheximide
P300	E1A-binding protein, 300 kDa
PCAF	P300/CBP-associated factor
CBP	CREB-binding protein

promotes ubiquitination to affect protein stability [9]. Deacetylation of PARP1, the regulatory mechanisms of PARP1 deacetylation, and the crosstalk of PARP1 post-translational modifications remain unclear.

The deacetylase SIRT2 is an important member of the Sirtuin family and involved in various biological processes by deacetylating various physiological substrates [10–14]. Although evidence suggests that SIRT2 is a protective factor against myocardial hypertrophy [15,16], the role of SIRT2 in oxidative stress-induced vascular injury and its regulatory substrates remains unclear.

In this study, we used proteomics to uncover the molecular interactions involved in oxidative stress-induced vascular injury. We identified SIRT2 as the main deacetylase of the Sirtuin family, which is involved in oxidative stress-induced vascular injury, and a new regulatory complex, SIRT2-WWP2-PARP1. Mechanistically, using mass spectrometry and coimmunoprecipitation, we found that PARP1 was a previously unknown physiological substrate of SIRT2. Moreover, SIRT2/CBP deacetylated/acetylated the PARP1-K249 residue. Furthermore, SIRT2 interacted with PARP1 at the PARP1-A-helical domain, which led to ubiquitination of the K249 residue of PARP1 via mobilization of the E3 ubiquitin ligase WWP2 and proteasome-mediated degradation of PARP1. Additionally, using SIRT2-knockout (KO) and SIRT2-transgenic (TG) mice and cells, we confirmed that SIRT2 protected against oxidative stress-induced vascular damage by deacetylation and ubiquitination of PARP1.

2. Materials and methods

2.1. SIRT2 knockout and transgenic mice

SIRT2-knockout (SIRT2-KO) mice were a kind gift from Deng CX [13] [Genetics of Development and Disease Branch, National Institute of Diabetes, Digestive and Kidney Diseases, National Institutes of Health (NIH)]. SIRT2-transgenic (SIRT2-TG) mice (CAG promoter) were provided by Shanghai Model Organisms Science & Technology Development. Effective knockdown and overexpression of SIRT2 were confirmed by western blotting (Figs. 5 and 6). Specific pathogen-free male mice (8–10 weeks old) were used in all mouse experiments. In the Ang II or NaCl infusion mouse model, SIRT2-WT, SIRT2-KO, and SIRT2-TG animals (n = 48 in total with n = 6/group) were randomized into groups, anesthetized with inhaled isoflurane/oxygen (2% at 1,500 ml/min), subjected to an incision in the middle scapular region, and subcutaneously implanted with an osmotic minipump (Alzet) in accordance with the manufacturer's instructions. To induce vascular damage and remodeling, mice were infused with Ang II (1.5 mg/kg/day) for 14 days delivered by the Alzet minipump (Alzet, model 2002; 0.5 μl/h) as described in our previous study [6]. After 14 days, the mice were euthanized by cervical dislocation. All animal experiments were approved by the Animal Subjects Committee of China Medical University (permission number: 2019026) and followed the Guide for the Care and Use of Laboratory Animals proposed by the US National Institutes of Health (NIH Publication No. 85-23, revised 1985).

2.2. Histopathological analysis

Vascular tissue specimens were fixed with 4% formalin for 4 h, embedded in paraffin, and cut into 5-μm-thick sections. The sections were then dewaxed with xylene, rehydrated with graded ethyl alcohol, and stained with H&E and Masson's trichrome stain solution (G1340; Solarbio, China). Vascular tissue specimens underwent frozen section and were followed by dihydroethidium (DHE) staining (C1300-2, Applygen Technologies Inc, China).

2.3. Cells and treatment

Human umbilical vein endothelial cells (HUVECs) were obtained from the ATCC, which had been tested for mycoplasma contamination, and cultured in F–12K medium with 10% fetal bovine serum (FBS) (HyClone), 0.1 mg/ml heparin, and 0.05 mg/ml endothelial cell growth supplement. HEK293T cells were obtained from the ATCC, which has been tested for mycoplasma contamination, and cultured in high-glucose Dulbecco's modified Eagle's medium with 10% FBS (HyClone). All cell culture was performed at 37 °C in a humid environment with 5% CO_2.

2.4. Reactive oxygen species (ROS) assay

A ROS Assay Kit was used to detect intracellular ROS (S0033, Beyotime Biotechnology, China). After the indicated treatment, HUVECs were washed three times with phosphate-buffered saline (PBS), suspended in 500 μl serum-free medium with 10 mM 2,7-DCFH-DA, and incubated for 1 h at 37 °C while protected from light. The cells were washed three times with PBS and then imaged under a fluorescence microscope (Olympus) at excitation of 595 nm.

2.5. TUNEL staining

The TUNEL assay was performed with a kit provided by Jiangsu KeyGEN BioTECH Co., Ltd. (China) in accordance with the manufacturer's instructions. After the indicated treatments, HUVECs were fixed with 4% formalin for 20 min. The cells were then permeabilized with 1% Triton X-100 for 10 min, followed by treatment with DNase I at 37 °C for 30 min, and subsequently washed three times with PBS. Prepared terminal deoxynucleotidyl transferase enzyme reaction drops were added to the samples and allowed to react at 37 °C for 60 min in the dark before the samples were washed three times with PBS. Streptavidin-fluorescein-labeled droplets were added to the samples and allowed to react at 37 °C for 30 min in the dark before the samples were again washed three times with PBS. The 4',6-diamidino-2-phenylindole staining solution was used to stain nuclei for 10 min at room temperature while protected from light. The cells were imaged under the fluorescence microscope at excitation of 488 nm.

2.6. Plasmid construction, antibodies, and reagents

Plasmids and knockdown shRNAs are shown in Supplementary Table 1. Plasmid transfection was conducted using Lipofectamine 3000 (Invitrogen, USA), Highgene (Applygen, China) or jetPRIME (Polyplus, France) in accordance with the manufacturer's protocol. shRNAs were transduced in a lentiviral vector. Antibodies are listed in Supplementary Table 2. Proteasome inhibitors MG132 (A2585) and cycloheximide (CHX) (A8244) were provided by Apexbio (USA) and dissolved in

dimethyl sulfoxide (DMSO). Ang II (A9525) was provided by Sigma (USA) and used at a concentration of 10 μM in DMSO.

2.7. PARP1 ubiquitination assessment

Vascular tissue specimens from mice and cells were lysed with 1% SDS buffer (Tris pH 7.5, 0.5 mM EDTA, and 1 mM DTT) and boiled for 10 min and saturated with Tris-HCL (pH 8.0). Cells that had been transfected with HA-tagged (HA)-ubiquitin, full-length human Myc-PARP1, mutant Myc-PARP1 plasmids, or other plasmids at 48 h prior were also lysed using the above protocol. Cell lysates were incubated at 4 °C with anti-PARP1 antibodies (1 μg antibody per mg of cell lysate), followed by incubation with 30 μl protein A/G (B23202; Biotool, USA) or anti-Myc (B26302; Biotool, USA) immunoprecipitation magnetic beads for 12 h.

2.8. Coimmunoprecipitation and immunoblotting

Vascular tissue specimens from mice and cells were each lysed with Flag lysis buffer [50 mM Tris, 137 mM NaCl, 1 mM ethylene diamine tetraacetic acid (EDTA), 10 mM NaF, 0.1 mM Na_3VO_4, 1% NP-40, 1 mM dithiothreitol (DTT), and 10% glycerol, pH 7.8] with protease inhibitors (Bimake). The lysates were incubated with 30 μl anti-Flag/Myc Affinity Gel (B23102/B26302; Biotool, USA) for 12 h at 4 °C or with appropriate antibodies (1 μg antibody per mg of cell lysate) for 2–3 h, after which the samples were incubated with 30 μl Protein A/G for immunoprecipitation (B23202; Bio tool) for 12 h at 4 °C. The immunoprecipitated complexes were separated by sodium dodecyl sulfate-polyacrylamide gel electrophoresis and electrotransferred onto PVDF membranes. After blocking with 5% bovine serum albumin for 1 h at ambient temperature, the specimens were successively incubated with primary (4 °C, overnight) and secondary (ambient conditions, 1 h) antibodies. Ubiquitinated PARP1 was immunoprecipitated using anti-Myc or anti-PARP1 antibodies and detected with an anti-HA antibody. GAPDH and Tubulin were concurrently assessed as loading controls. ImageJ v1.46 (National Institutes of Health, USA) was used for quantitation.

2.9. Statistical analysis

Data are presented as the mean ± standard deviation (SD) and were assessed for homogeneity of variance by the F-test and Brown–Forsythe test for group pairs and multiple groups, respectively. Data normality was examined by the Shapiro–Wilk test. Student's and Welch's t-tests were applied for data with equal and unequal variances, respectively (group pairs). One- and two-way ANOVAs were performed to assess differences in multiple groups, which involved one and two factors, respectively, with a Bonferroni post-hoc test. P-value adjustment was performed for multiple comparisons as appropriate. Data analysis was carried out using SPSS 22.0 (SPSS, USA) with $P < 0.05$ deemed statistically significant.

3. Results

3.1. Mass spectrometric analyses of SIRT2-interacting proteins identifies PARP1 as a novel physiological substrate of SIRT2

To identify the major deacetylase activity involved in vascular injury, we examined Sirtuin isoform expression profiles following damage from vascular injury induced in wildtype (WT) mice via Ang II infusion. We conducted iTRAQ/TMT/label-free analysis and further quantification of the expression levels of Sirtuin isoform proteins was performed by LC-PRMMS analysis performed by Shanghai Applied Protein Technology Co., Ltd [17]. Among the seven Sirtuin isoform proteins, SIRT2 was the most highly upregulated in injured vessels after 14 days of Ang II infusion (Fig. 1A). These results suggested that SIRT2 may play a major role in vascular injury.

SIRT2 is a deacetylase, and therefore we hypothesized that SIRT2 may deacetylate a novel physiological substrate to act in vascular dysfunction. To this end, we identified SIRT2-interacting partners. SIRT2 was expressed and purified, followed by mass spectroscopic analysis to identify interacting partners. Furthermore, Gene Ontology, Biological Process, Molecular Function and Cellular Component enrichment analysis revealed that these molecules were involved in the cellular process, biological regulation, and protein binding (Fig. 1B–E). Thus, we identified that injury factor PARP1 was the major novel interacting protein of SIRT2. Next, the interaction between purified SIRT2 and PARP1 was confirmed by mass spectrometry (Fig. 1F). The interaction between endogenous SIRT2 and PARP1 was assessed by performing coimmunoprecipitation assays (Fig. 1G and H). Furthermore, we found that SIRT2 is bound to the 662–779 amino acid domain of PARP1, namely the PARP-A-helical domain (Fig. 1I). These results suggested that the SIRT2-PARP1 axis was a novel regulatory factor in the vascular damage pathway.

3.2. SIRT2/CBP deacetylation/acetylation of PARP1 acts on PARP1-K249

As a deacetylase, SIRT2 was assumed to bind to and deacetylate PARP1. Therefore, we first confirmed by immunoprecipitation that PARP1 was acetylated and that its acetylation status was regulated by trichostatin A (TSA) and nicotinamide (NAM), two frequently used deacetylase inhibitors that repress histone deacetylases (HDACs), which include HDAC I and III as well as the Sirtuin family of deacetylases (Fig. 2A). Among the four common acetyltransferases, P300 (E1A-binding protein, 300 kDa), CREB-binding protein (CBP), P300/CBP-associated factor (PCAF), and GCN5 (KAT2A), we found that CBP, but not the other three acetyltransferases, markedly enhanced PARP1 acetylation (Fig. 2B). We also confirmed an interaction between CBP and PARP1 (Fig. 2C and D). These results confirmed that PARP1 underwent acetylation and CBP was the acetyltransferase of PARP1.

Next, we determined whether the presence of SIRT2 affected the levels of PARP1 acetylation. Indeed, SIRT2-WT, but not SIRT2-Q167AH187Y (SIRT2 inactivation mutation), significantly reduced PARP1 acetylation (Fig. 2E). Moreover, the acetylation levels of PARP1 were higher in shSIRT2-treated cells using the 22297 shSIRT2 fragment, which had the optimal SIRT2 knockdown efficiency, and in SIRT2 inhibitor (AGK2)-treated cells compared with control-treated cells (Fig. 2F). Thus, SIRT2 regulated PARP1 via deacetylation, which further supported the conclusion that PARP1 was a novel physiological substrate of SIRT2.

To obtain the most direct evidence of the PARP1 modification by deacetylation through SIRT2, we investigated the specific PARP1 site deacetylated by SIRT2. We mutated each of seven identified putative acetylation sites in PARP1, i.e. K105, K108, K249, K254, K400, K418, K600, and K621, and analyzed acetylation by mass spectrometry. Each lysine (K) residue was changed to arginine (R), which produced non-acetylated mutants. Only the mutation of lysine (K) 249 residue to R decreased the levels of PARP1 acetylation, and the arginine substitution of K249 resulted in minimal differences in the levels of PARP1 acetylation in the presence or absence of SIRT2 overexpression (Supplementary Figs. 1A and B). We then co-transfected cells with WT-PARP1 or mutant PARP1-K249R plasmids and the Flag control or Flag-CBP plasmid. The arginine substitution of K249R blunted PARP1 acetylation with or without CBP expression, whereas the acetylation levels of WT-PARP1 were increased in the presence of additional CBP (Fig. 2G). In agreement with these findings, compared with the PARP1-WT group, transfection with the mutant PARP1-K249R plasmid suppressed PARP1 acetylation. Co-transfection with the SIRT2 plasmid decreased the acetylation levels of WT-PARP1, whereas the acetylation levels of PARP1-K249R were unchanged in the presence of additional SIRT2 (Fig. 2H). PARP1-K249 acetylation was further assessed using an antibody that specifically recognized ectopically expressed WT-PARP1, but

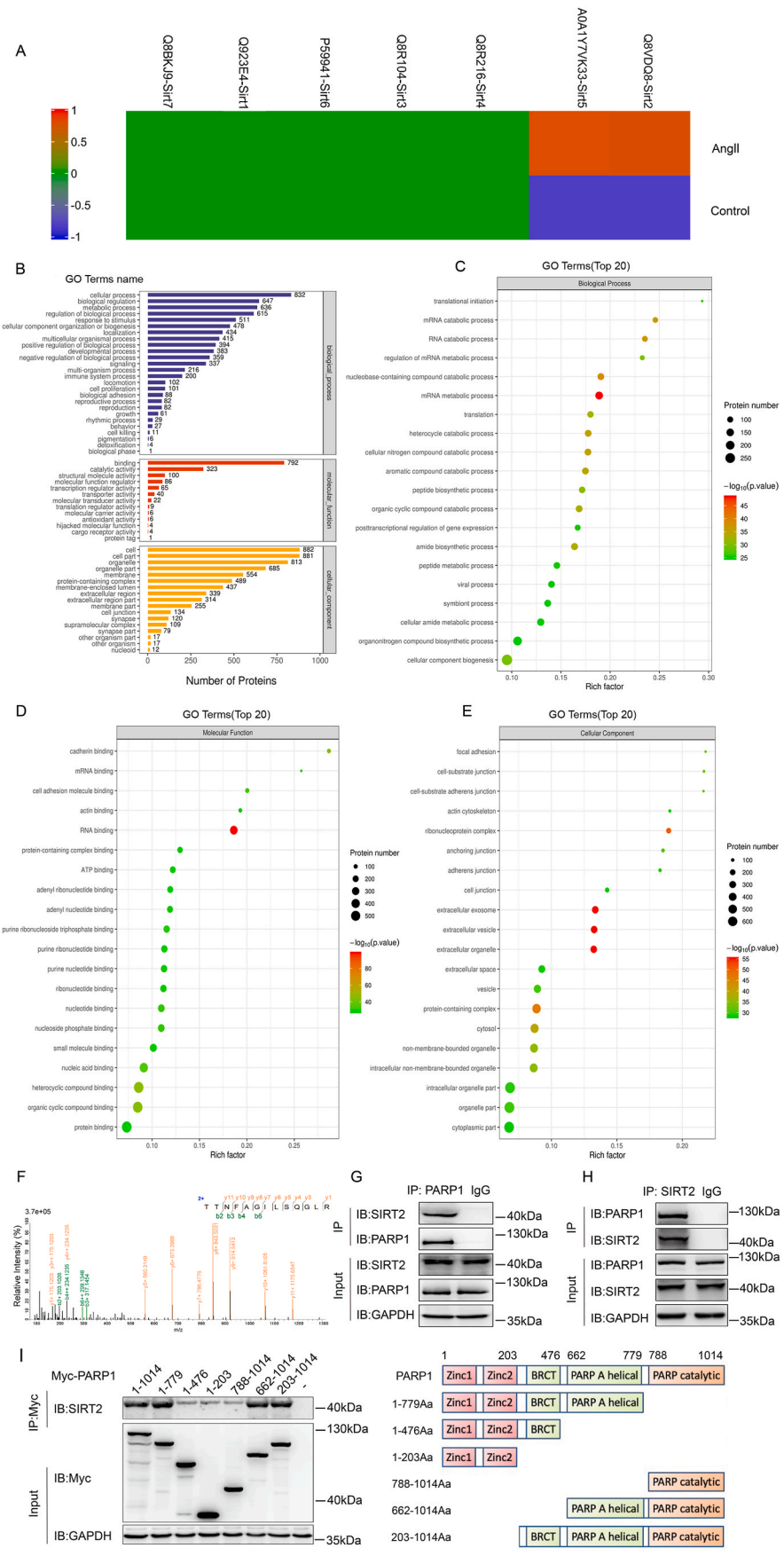

Fig. 1. Mass spectrometric analyses of SIRT2-interacting proteins identifies PARP1 as a novel physiological substrate of SIRT2. (**A**) Vascular injury was induced in WT mice via Ang II infusion and Sirtuin isoform expression levels were analyzed by iTRAQ/TMT/label-free analysis. The expression levels of Sirtuin isoform proteins were then further quantified by LC-PRMMS analysis. (**B**) Identification of SIRT2-interacting proteins by mass spectrometric analysis. The results from mass spectrometric analysis of SIRT2-interacting proteins were analyzed by Gene Ontology term enrichment. The most significant pathways associated with protein binding are shown. P-values were calculated using Fisher's exact test. (**C–E**) Biological Process, Molecular Function, and Cellular Component enrichment analysis of SIRT2-interacting proteins. P-values were calculated using Fisher's exact test. (**F**) Interaction between purified Flag-SIRT2 and PARP1 analyzed by mass spectroscopy. (**G**) Endogenous PARP1 and SIRT2 immunoprecipitated using an anti-PARP1 antibody and detected with an anti-SIRT2 antibody. (**H**) Endogenous SIRT2 and PARP1 immunoprecipitated using an anti-SIRT2 antibody and detected with an anti-PARP1 antibody. (**I**) Full length Myc-PARP1 or one of six truncated Myc-PARP1 plasmids were transfected and total lysates were subjected to immunoprecipitation with an anti-Myc antibody, followed by western blotting with an anti-SIRT2 antibody.

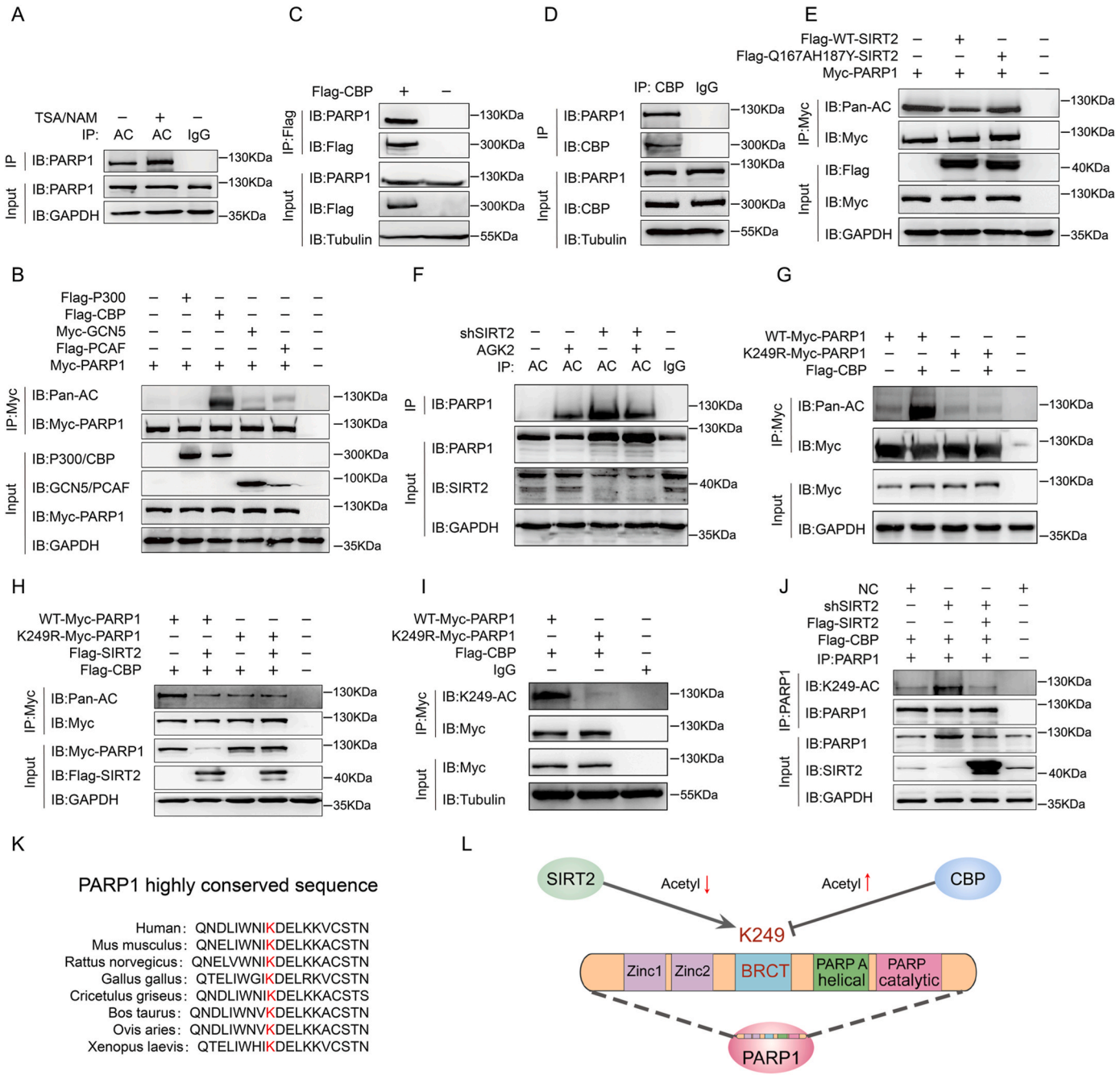

Fig. 2. Modification of PARP1 by SIRT2/CBP deacetylation/acetylation acts on PARP1-K249. (**A**) Cells treated with nicotinamide (NAM) (5 mM, 4 h) and trichostatin A (TSA) (0.5 μM, 16 h) were lysed and immunoprecipitated using an anti-Pan-AC antibody, followed by detection with an anti-PARP1 antibody. (**B**) Cells cotransfected with Myc-P300, Myc-GCN5, Flag-CBP, or Flag-P300/CBP-associated factor (PCAF) and Myc-PARP1 were lysed and acetylated PARP1 was immunoprecipitated using an anti-Myc antibody and detected with an anti-Pan-AC antibody. (**C**) Flag-CBP-transfected cells were lysed and exogenous Flag-CBP was immunoprecipitated using an anti-Flag antibody and detected with anti-PARP1 antibody. (**D**) Cells were lysed and endogenous CBP was immunoprecipitated using an anti-CBP antibody and detected with an anti-PARP1 antibody. (**E**) Cells cotransfected with Flag-WT-SIRT2 or Flag-SIRT2-H187YQ167A (Mut) and Myc-PARP1 were lysed and acetylated PARP1 was immunoprecipitated using an anti-Myc antibody and detected with an anti-Pan-AC antibody. (**F**) NC and shSIRT2 cells that were subsequently treated with or without AGK2 (20 μM, 24 h) were subjected to immunoprecipitation using an anti-Pan-AC antibody. Acetylated PARP1 was then detected with an anti-PARP1 antibody. (**G–H**) Cells cotransfected with Myc-WT-PARP1 or Myc-PARP1-K249R (Mut) and Flag-CBP alone (**G**) or Flag-SIRT2 (**H**) were lysed and acetylated PARP1 was immunoprecipitated using an anti-Myc antibody and detected using an anti-Pan-AC antibody. (**I**) Cells cotransfected with Myc-WT-PARP1 or Myc-PARP1-K249R (Mut) and Flag-CBP were lysed and acetylated PARP1 was immunoprecipitated using an anti-Myc antibody and detected with the site-specific anti-K249 acetylation antibody (PARP1-K249AC). (**J**) Flag-SIRT2 was transfected into NC or shSIRT2 cells and PARP1 acetylation was detected by immunoprecipitation using the anti-PARP1-K249AC antibody. (**K**) Alignment of sequences that surround K249 in PARP1 homologs of various species. The acetylated lysine residues at PARP1-249 are shown in bold red text. (**L**) Schematic model of the proposed role of SIRT2 in deacetylating PARP1. (For interpretation of the references to colour in this figure legend, the reader is referred to the Web version of this article.)

not the mutant PARP1-K249R (Fig. 2I). Additionally, compared with the NC cells, the levels of K249-acetylated PARP1 were increased in shSIRT2-treated cells, whereas the levels of K249-acetylated PARP1 were restored in shSIRT2-treated cells that were transfected with Flag-SIRT2, which confirmed that SIRT2 regulated PARP1-K249 deacetylation (Fig. 2J). Furthermore, PARP1-K249 was found to be highly conserved in mammals (Fig. 2K).

Overall, the above results confirmed that SIRT2 interacted with the PARP-A-helical domain of PARP1 and that CBP and SIRT2 acetylated and deacetylated PARP1-K249, respectively. These findings provided crucial insights into the regulatory mechanism of the SIRT2-PARP1 complex (Fig. 2L).

3.3. SIRT2 promotes PARP1-K249 ubiquitination by the E3 ubiquitin ligase WWP2

Lysine acetylation of non-histone proteins competes with ubiquitination to affect protein stability [9], and therefore we next examined the effect of SIRT2 expression on PARP1 levels. We found that increasing levels of SIRT2 overexpression led to a gradual reduction in PARP1 levels (Fig. 3A). Conversely, knockdown of SIRT2 using the 22297 shSIRT2 RNA fragment markedly upregulated PARP1 levels (Fig. 3B). Moreover, we found that expression of mutant SIRT2-Q167AH187Y did not affect PARP1 levels (Fig. 3C). We then determined whether SIRT2 affected PARP1 transcription or its stability. The results showed that NC cells displayed substantially lower levels of PARP1 in a post-CHX treatment time course, whereas the shSIRT2 group maintained very high levels of PARP1 over time (Fig. 3D). Moreover, the rate and extent of the PARP1 levels increase were higher after MG132 treatment of NC cells compared with those observed in shSIRT2 cells (Fig. 3E). Furthermore, PARP1 levels had gradually declined in the Flag control group, whereas the SIRT2 overexpression group had a faster declining rate of PARP1 levels (Fig. 3F). These results suggested that SIRT2 promoted degradation of PARP1 via a proteasome pathway. Additionally, after MG132 treatment, both the rate and proportion of the PARP1 levels increase were elevated in SIRT2-overexpressing cells compared with Flag control group cells (Fig. 3G). Therefore, our results showed that SIRT2 expression caused a decrease in PARP1 by inducing proteasomal degradation of PARP1. Consistent with degradation through the ubiquitin-proteasome pathway, compared with the Flag-control plasmid group, the PARP1 ubiquitination levels were increased by overexpression of Flag-SIRT2 (Fig. 3H). Furthermore, in shSIRT2-treated cells, the levels of PARP1 polyubiquitination by the E3 ubiquitin ligase WWP2 were lower than that in NC-treated cells (Fig. 3I). Additionally, overexpression of Flag-SIRT2 enhanced the interaction between PARP1 and the E3 ubiquitin ligase WWP2 (Fig. 3J). These results further showed that SIRT2 promoted ubiquitination of PARP1 by the E3 ubiquitin ligase WWP2.

To obtain the most direct evidence that SIRT2 promoted ubiquitination of PARP1 by the E3 ubiquitin ligase WWP2, we identified ubiquitination sites in PARP1 regulated by SIRT2. The results showed that SIRT2 increased the ubiquitination levels of PARP1-WT, but not PARP1-K249R, which proved that SIRT2 promoted the ubiquitination of PARP1 via K249 (Fig. 3K).

Taken together, these results revealed that SIRT2 promoted PARP1 ubiquitination by deacetylating PARP1-K249 to induce PARP1 polyubiquitination by the E3 ubiquitin ligase WWP2, which further supported the regulatory role of the SIRT2–PARP1 complex (Fig. 3L).

3.4. SIRT2 significantly decreases PARP1-K249 acetylation and increases PARP1 ubiquitination in Ang II-treated HUVECs

PARP1 is a major damaging factor in vascular injury [4,5] and our results delineated complex regulatory behavior of SIRT2-PARP1, and therefore we next examined the role of this complex in an Ang II-induced HUVEC injury model. First, considering the physical interaction of SIRT2 with PARP1, we assessed whether Ang II affected the interaction between SIRT2 and PARP1 in HUVECs. As expected, Ang II stimulation increased the interaction between SIRT2 and PARP1 (Fig. 4A and B). Second, compared with the NC group, SIRT2 knockdown increased PARP1-K249 acetylation in HUVECs and Ang II stimulation of SIRT2 knockdown HUVECs further increased PARP1-K249 acetylation (Fig. 4C). Third, under Ang II stimulation, SIRT2 knockdown decreased the PARP1 ubiquitination levels, and the re-expression of SIRT2 in shSIRT2-treated cells increased the PARP1 ubiquitination levels (Fig. 4D).

Finally, the results showed that in NC HUVEC cells, in shSIRT2-treated HUVEC cells, and also in shSIRT2-treated HUVEC cells transfected with Flag-SIRT2, Ang II stimulation significantly increased PARP1 and Cleaved-Caspase3 proteins levels (###, $P < 0.001$) (Fig. 4E), and oxidative stress markers 3-Nitrotyrosine and OGG1 proteins levels, and significantly decreased anti-oxidative stress marker SOD1 protein levels (###, $P < 0.001$; #, $P < 0.05$) (Fig. 4F), and significantly increased ROS production (###, $P < 0.001$) (Fig. 4G), and cell apoptosis (###, $P < 0.001$) (Fig. 4H).

In addition, SIRT2 knockdown significantly increased the protein levels of Ang II-induced PARP1 and Cleaved-Caspase3 (***, $P < 0.001$) (Fig. 4E), as well as the levels of oxidative stress markers 3-Nitrotyrosine and OGG1. It also significantly decreased Ang II-induced antioxidative stress marker SOD1 protein levels (***, $P < 0.001$; **, $P < 0.01$) (Fig. 4F) and significantly increased ROS production (**, $P < 0.01$) (Fig. 4G) and cell apoptosis (**, $P < 0.01$) (Fig. 4H). However, re-expression of SIRT2 in shSIRT2-treated cells significantly decreased the proteins levels of Ang II-induced PARP1 and Cleaved-Caspase3 (***, $P < 0.001$) (Fig. 4E), as well as the levels of oxidative stress markers 3-Nitrotyrosine and OGG1. It also significantly increased Ang II-induced anti-oxidative stress marker SOD1 protein levels (***, $P < 0.001$; **, $P < 0.01$) (Fig. 4F) and significantly decreased ROS production (*, $P < 0.05$) (Fig. 4G) and cell apoptosis (**, $P < 0.01$) (Fig. 4H).

Taken together, these in vitro findings confirmed that SIRT2 decreased PARP1-K249 acetylation and increased PARP1 ubiquitination in the Ang II-induced HUVEC injury model.

3.5. SIRT2 knockout significantly aggravates Ang II-induced vascular injury and remodeling by increasing PARP1-K249 acetylation and PARP1 levels in mice

Next, we conducted experiments in SIRT2-KO mice to verify the interaction between SIRT2 and PARP1 (Fig. 5A). The results showed that both in SIRT2-WT and SIRT2-KO mice, Ang II stimulation significantly induced vascular thickening after vascular injury (###, $P < 0.001$; ##, $P < 0.01$) (Fig. 5B), vascular fibrosis (###, $P < 0.001$) (Fig. 5C), and vascular ROS generation (###, $P < 0.001$) (Fig. 5D), and significantly elevated expression of PARP1 acetylated at site K249 (PARP1-K249AC) (##, $P < 0.01$; #, $P < 0.05$) (Fig. 5E), and significantly elevated expression of PARP1 and Cleaved-Caspase3 (###, $P < 0.001$) (Fig. 5F), and markedly increased the expression of oxidative stress markers 3-Nitrotyrosine and OGG1, and had significantly decreased the expression of anti-oxidative stress marker SOD1 (###, $P < 0.001$) (Fig. 5G).

In addition, in the model of Ang II-induced vascular injury and post-injury vascular remodeling, compared with the SIRT2-WT group, SIRT2-KO mice displayed significantly aggravated vascular thickening after vascular injury (***, $P < 0.001$) (Fig. 5B), vascular fibrosis (***, $P < 0.001$) (Fig. 5C), and vascular ROS generation (**, $P < 0.01$) (Fig. 5D). Furthermore, through site-specific antibody detection, we found that compared with the SIRT2-WT group, SIRT2-KO mice showed significantly elevated Ang II-induced expression of PARP1 acetylated at site K249 (PARP1-K249AC) (***, $P < 0.001$) (Fig. 5E). Additionally, SIRT2-KO mice showed markedly higher amounts of Ang II-associated vascular injury proteins PARP1 and Cleaved-Caspase3 (*, $P < 0.05$) (Fig. 5F). Compared with the SIRT2-WT group, SIRT2-KO mice had markedly increased expression of Ang II-induced oxidative stress markers 3-

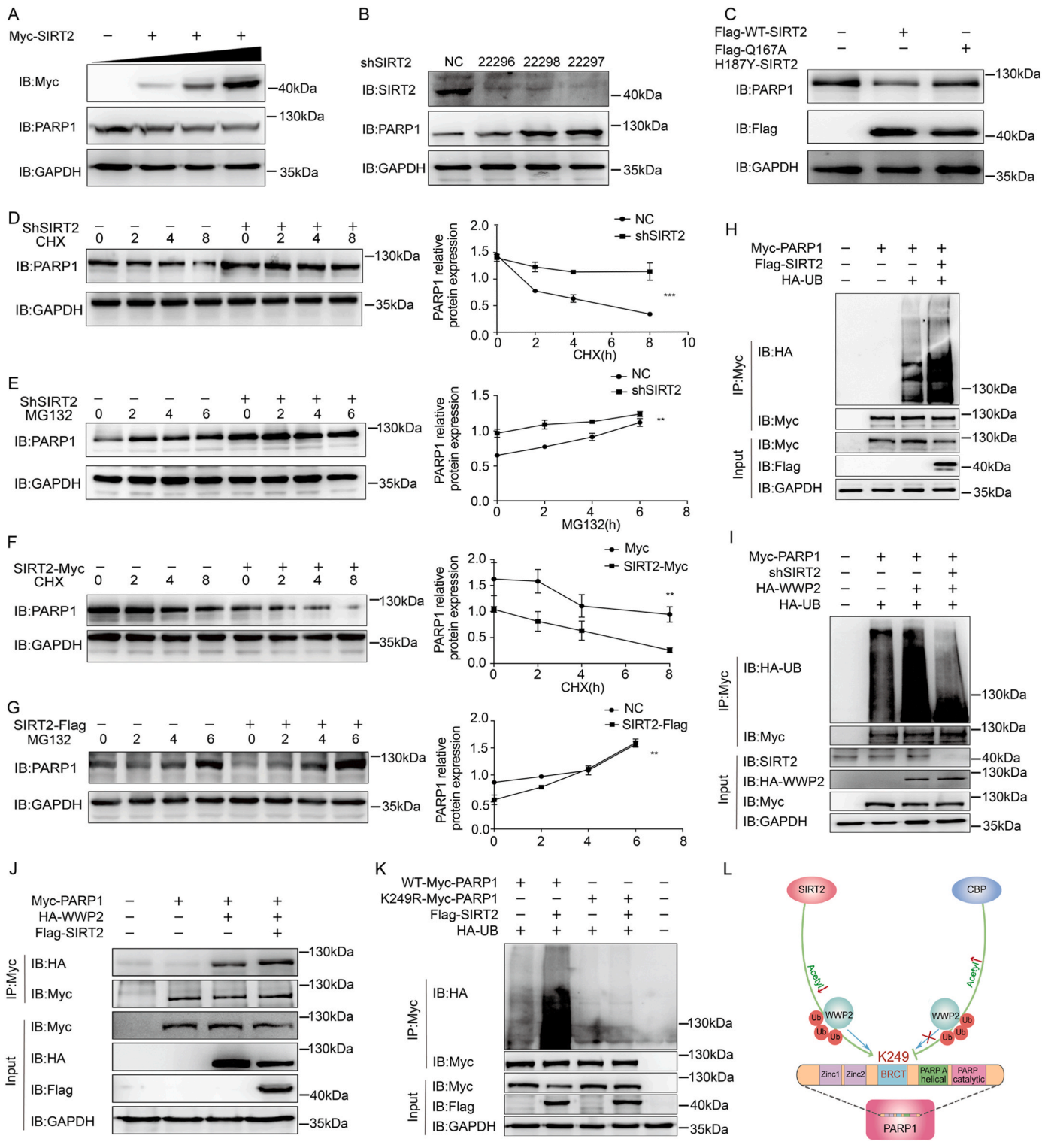

(caption on next page)

Fig. 3. SIRT2 promotes PARP1-K249 ubiquitination by the E3 ubiquitin ligase WWP2.
(**A**) Various concentrations of Myc-SIRT2 plasmid were transfected and the levels of PARP1 were examined by western blotting. (**B**) Expression levels of SIRT2 were measured in NC, shSIRT2-22296, shSIRT2-22298, or shSIRT2-22297 cells. (**C**) Flag-WT-SIRT2 or Flag-SIRT2-H187YQ167A (Mut) were transfected and the levels of PARP1 were detected by western blotting. (D) NC and shSIRT2 cells were subsequently treated with CHX for the indicated times and the levels of PARP1 were examined by western blotting (each experiment was repeated three times, ***P < 0.001). (**E**) NC and shSIRT2 cells were subsequently treated with MG132 for the indicated times and the levels of PARP1 were examined by western blotting (each experiment was repeated three times, **P < 0.01). (**F**) Flag-control and Flag-SIRT2 cells were subsequently treated with CHX for the indicated times and the levels of PARP1 were examined by western blotting (each experiment was repeated three times, **P < 0.01). (**G**) Flag-control and Flag-SIRT2 cells were subsequently treated with MG132 for the indicated times and the levels of PARP1 were examined by western blotting (each experiment was repeated three times, **P < 0.01). (**H**) Cells were cotransfected with Myc-PARP1, Flag-SIRT2, and HA-UB, and ubiquitinated PARP1 was immunoprecipitated using an anti-Myc antibody and detected with an anti-HA antibody. (**I**) NC and shSIRT2 cells were cotransfected with Myc-PARP1, HA-WWP2, and HA-UB, and ubiquitinated PARP1 was immunoprecipitated using an anti-Myc antibody and detected with an anti-HA antibody. (**J**) Cells were cotransfected with Myc-PARP1, HA-WWP2, and Flag- SIRT2, and the interaction complex of exogenous PARP1 and WWP2 was immunoprecipitated using an anti-Myc antibody and detected with an anti-HA antibody. (**K**) Cells were cotransfected with Flag-SIRT2, HA-UB, and either Myc-WT-PARP1 or Myc-PARP1-K249R (Mut) and ubiquitinated PARP1 was immunoprecipitated using an anti-Myc antibody and detected with an anti-HA antibody. (**L**) Schematic model of the proposed role of PARP1 deacetylation by SIRT2 to induce PARP1 polyubiquitination by the E3 ubiquitin ligase WWP2.

Nitrotyrosine and OGG1, and significantly decreased expression of the Ang II-induced antioxidative stress marker SOD1 (***, P < 0.001; **, P < 0.01) (Fig. 5G).

These in vivo results confirmed that SIRT2-KO increased PARP1-K249 acetylation and PARP1 levels, and aggravated Ang II-induced vascular oxidative stress injury and remodeling.

3.6. SIRT2 overexpression significantly relieves Ang II-induced vascular injury and remodeling by decreasing PARP1-K249 acetylation and PARP1 levels in mice

Finally, we conducted experiments in SIRT2-TG mice to verify the interaction between SIRT2 and PARP1 (Fig. 6A). The results showed that Ang II stimulation significantly induced vascular thickening after vascular injury (##, P < 0.01) (Fig. 6B), vascular fibrosis (###, P < 0.001) (Fig. 6C), and vascular ROS generation (###, P < 0.001) (Fig. 6D) in both SIRT2-WT and SIRT2-TG mice. And Ang II stimulation significantly elevated expression of PARP1 acetylated at site K249 (PARP1-K249AC) in SIRT2-WT mice (#, P < 0.05) (Fig. 6E), and significantly elevated expression of PARP1 and Cleaved-Caspase3 in SIRT2-WT mice (###, P < 0.001; ##, P < 0.01) (Fig. 6F). And Ang II stimulation markedly increased the expression of oxidative stress markers 3-Nitrotyrosine and OGG1, and had significantly decreased the expression of anti-oxidative stress marker SOD1 in both SIRT2-WT and SIRT2-TG mice (###, P < 0.001; ##, P < 0.01; #, P < 0.05) (Fig. 6G).

In addition, in the model for Ang II-induced vascular injury and post-injury vascular remodeling, compared with the SIRT2-WT group, SIRT2-TG mice displayed significantly reduced vascular thickening after vascular injury (***, P < 0.001) (Fig. 6B), vascular fibrosis (***, P < 0.001) (Fig. 6C), and vascular ROS generation (***, P < 0.001) (Fig. 6D). Furthermore, through site-specific antibody detection, we found that compared with the SIRT2-WT group, SIRT2-TG mice showed significantly reduced Ang II-induced expression of PARP1 acetylated at site K249 (PARP1-K249AC) (**, P < 0.01) (Fig. 6E). Additionally, SIRT2-TG mice showed markedly lower amounts of Ang II-associated vascular injury proteins PARP1 and Cleaved-Caspase3 (***, P < 0.001; **, P < 0.01) (Fig. 6F). Compared with the SIRT2-WT group, SIRT2-TG mice had markedly decreased expression of Ang II-induced oxidative stress markers 3-Nitrotyrosine and OGG1, and significantly increased expression of the Ang II-induced antioxidative stress marker SOD1 (**, P < 0.01; *, P < 0.05) (Fig. 6G).

These in vivo confirmed that SIRT2-TG decreased PARP1-K249 acetylation and PARP1 levels, and relieved Ang II-induced vascular oxidative stress injury and remodeling.

4. Discussion

In the present study, through proteomics and mass spectrometric analysis, we identified a novel modification complex (SIRT2-WWP2-PARP1). We found that the deacetylase SIRT2 is the main Sirtuin family factor involved in this process and identified the injury factor PARP1 as a new physiological substrate of SIRT2. SIRT2 interacts with PARP1, affects the PARP-A-helical domain, and deacetylates the K249 residue of PARP1 (Schematic model 1). SIRT2 deacetylates PARP1 and promotes ubiquitination of PARP1-K249 via mobilization of the E3 ubiquitin ligase WWP2, which leads to proteasome-mediated degradation of PARP1 (Schematic model 2). The in vitro experiments confirmed that SIRT2 decreased PARP1-K249 acetylation and increased PARP1 ubiquitination in the Ang II-induced HUVEC injury model. Additionally, the in vivo experiments confirmed that SIRT2-KO/SIRT2-TG increased/decreased PARP1-K249 acetylation and PARP1 levels in the Ang II-induced mouse injury model. Therefore, the discovery of the novel modification complex SIRT2-WWP2-PARP1 provides new insights into potential treatment strategies for vascular disease at the mechanistic, cellular, and animal levels.

PARP1 has major regulatory roles in oxidative stress and cardiovascular disease occurrence and development [4–8]. However, improvement of the clinical outcomes of cardiovascular disease by inhibiting PARP1 activity is not significant and has some side effects. Therefore, we need to increase our understanding of the mechanisms of cardiovascular disease checkpoint pathways. Our previous study revealed that PARP1 as the main oxidative stress factor in cardiovascular injury undergoes ubiquitination by E3 ubiquitin ligase WWP2 [6,7]. In the present study, we found that SIRT2 bound to PARP1 through the PARP-A-helical domain, deacetylated PARP1 at K249, and then promoted ubiquitination of PARP1-K249 via mobilization of the E3 ubiquitin ligase WWP2, which led to proteasome-mediated degradation of PARP1.

As an NAD^+-dependent deacetylase, SIRT2 plays roles in various biological processes that include lipid and glucose homeostasis, tumor suppression, and neurodegenerative diseases [10–14]. Interestingly, we found that SIRT2 protected against vascular damage through the SIRT2-WWP2-PARP1 pathway. Once PARP1 receives a message that indicates DNA damage, it forms a homodimer and catalyzes the degradation of NAD^+. For example, in advanced heart failure, excessive PARP1 activation reduces the levels of myocardial NAD^+ and ATP, which ultimately leads to myocardial cell necrosis [18,19].

Notably, SIRT2 exerted a protective effect against vascular damage induced by Ang II both in vivo and in vitro, which was dependent on the negative regulation of PARP1 by SIRT2. Ang II causes PARP1 overactivation through continuous and excessive oxidative stress, which

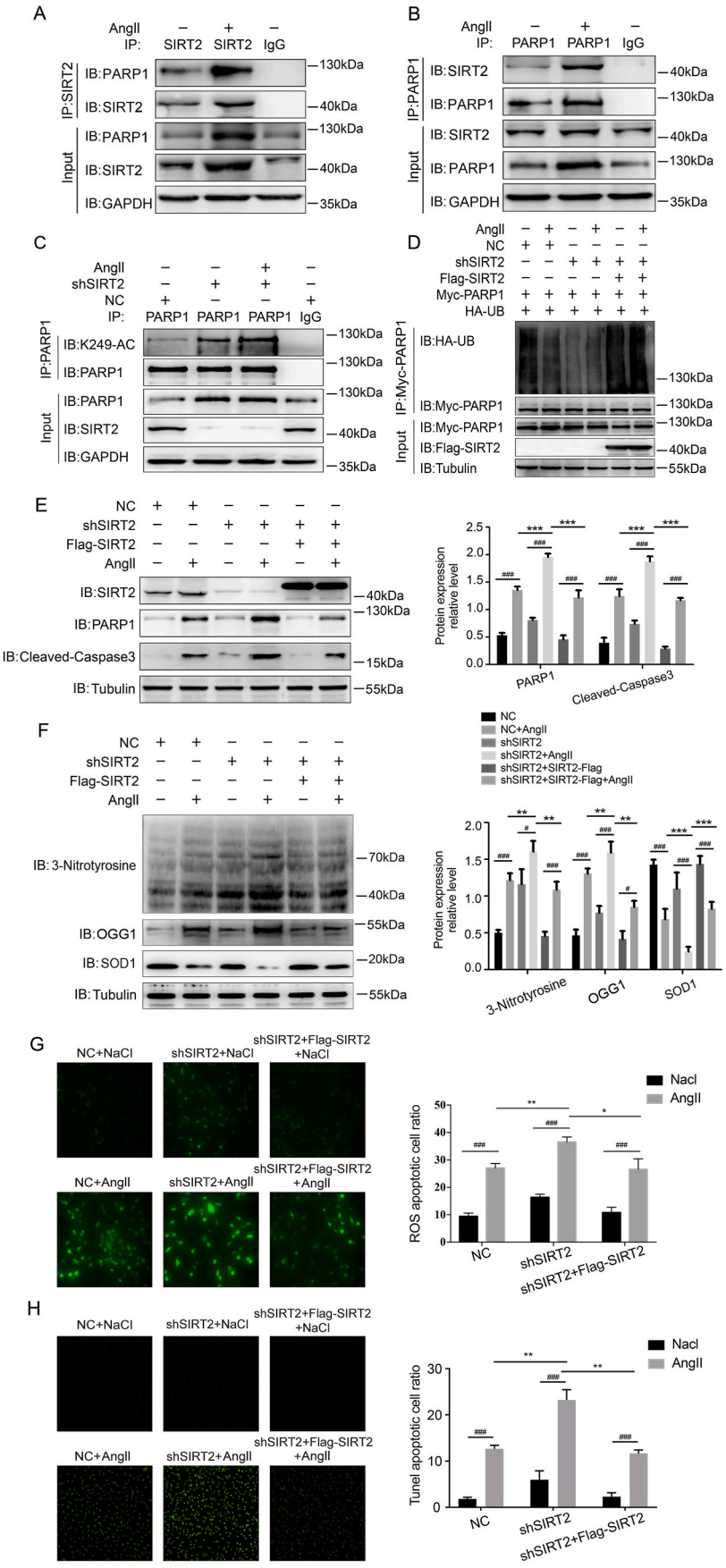

Fig. 4. SIRT2 significantly decreases PARP1-K249 acetylation and increases PARP1 ubiquitination in an Ang II-induced HUVEC injury model

(**A, B**) HUVECs were treated with NaCl or Ang II as indicated. The interaction between SIRT2 and PARP1 was detected by immunoprecipitation and western blotting using anti-SIRT2 and anti-PARP1 antibodies. (C) ShSIRT2 HUVECs were treated with NaCl or Ang II. PARP1 acetylation was detected by immunoprecipitation using anti-PARP1 beads and western blotting using an anti-PARP1-K249AC antibody. (**D**) HUVECs were cotransfected with Myc-PARP1 and HA-UB, and shSIRT2 HUVECs were cotransfected with Flag-SIRT2, Myc-PARP1, and HA-UB. These cells were then treated with NaCl or Ang II as indicated. Ubiquitinated Myc-PARP1 was detected by immunoprecipitation using anti-Myc beads and western blotting using an anti-HA antibody. (**E**) ShSIRT2 HUVECs were transfected with Flag-SIRT2 and then treated with Ang II or NaCl as indicated. Expression of SIRT2, PARP1, and Cleaved-Caspase3 was detected by western blotting using the indicated antibodies (each experiment was repeated three times, $^{\#\#\#}P < 0.001$, $^{***}P < 0.001$). (**F**) ShSIRT2 HUVECs were transfected with Flag-SIRT2 and then treated with Ang II or NaCl as indicated. 3-Nitrotyrosine, OGG1, and SOD1 were detected by western blotting using the indicated antibodies (each experiment was repeated three times, $^{\#}P < 0.05$, $^{\#\#\#}P < 0.001$, $^{**}P < 0.01$, $^{***}P < 0.001$). (**G, H**) ROS analysis and TUNEL staining were performed in Ang II or NaCl-treated HUVECs, shSIRT2 HUVECs, and shSIRT2 HUVECs that overexpressed Flag-SIRT2 (each experiment was repeated three times, $^{\#\#\#}P < 0.001$, $^{*}P < 0.05$, $^{**}P < 0.01$).

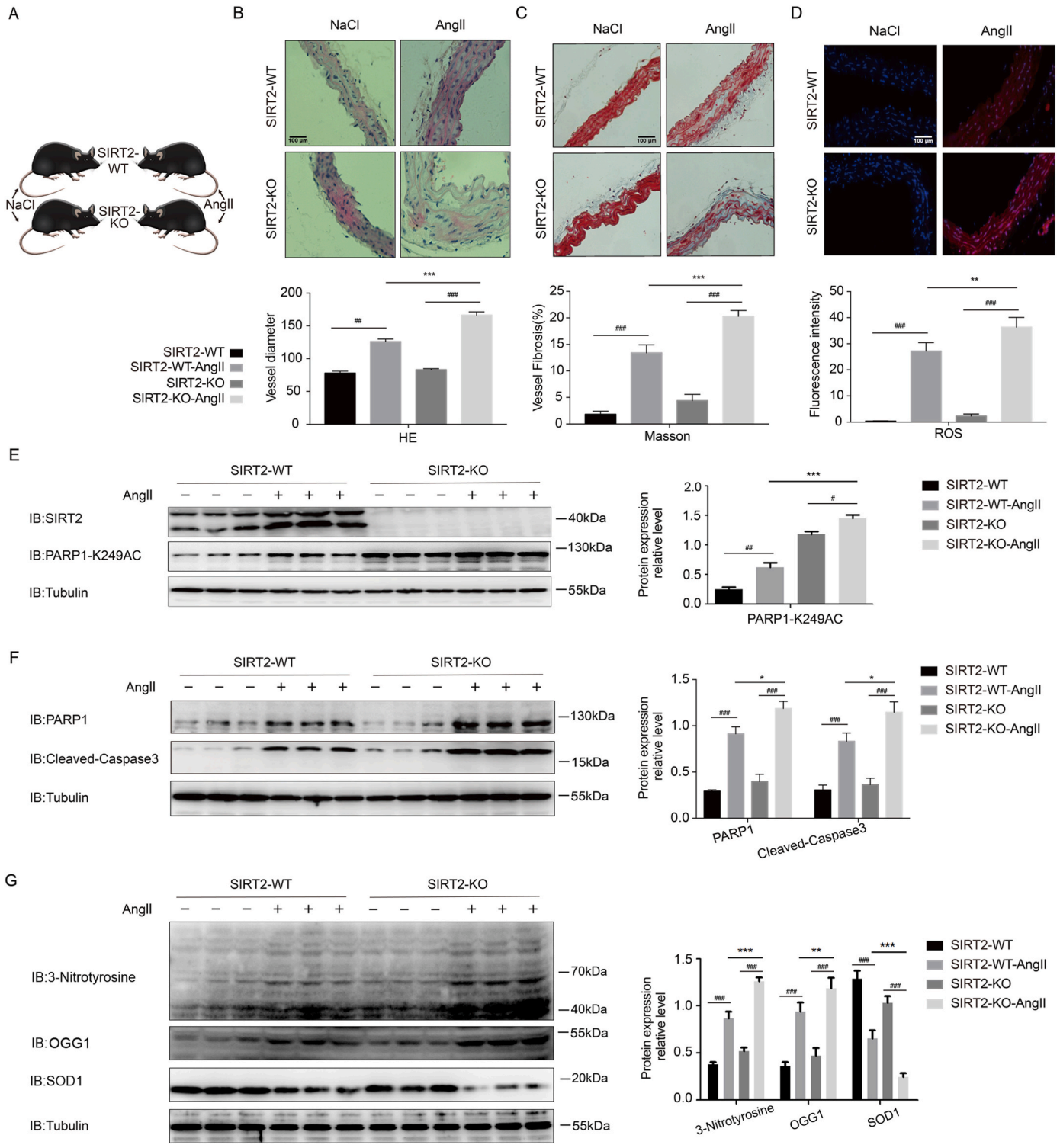

Fig. 5. SIRT2 knockout significantly aggravated Ang II-induced vascular injury and remodeling by increasing PARP1-K249 acetylation and PARP1 levels in mice. (**A**) SIRT2-WT and SIRT2-KO mice were treated with either the control (NaCl) or Ang II (1.5 mg/kg/day) administered via a subcutaneously implanted osmotic minipump (Alzet, model 2002; 0.5 μl/h) for 14 days. Mice were euthanized by cervical dislocation after 14 days of treatment. (**B**) H&E staining, (**C**) Masson staining, and (**D**) DHE staining were performed to assess the degree of vascular thickening, vascular fibrosis, and vascular ROS production, respectively. Scale bar, 100 μm. Data are expressed as means ± SD ($^{\#\#}P < 0.01$, $^{\#\#\#}P < 0.001$, $^{**}P < 0.01$, $^{***}P < 0.001$ for each group of mice, n = 6). (E) Total protein was obtained from the vascular tissue of SIRT2-WT and SIRT2-KO mice after infusion with either NaCl or Ang II for 14 days. Western blotting was performed to assess SIRT2 and PARP1-K249AC, or (**F**) PARP1 and Cleaved-Caspase3 expression levels as well as (**G**) 3-Nitrotyrosine, OGG1, and SOD1 expression levels. Quantification of western blot data is shown as the mean ± SD ($^{\#}P < 0.05$, $^{\#\#}P < 0.01$, $^{\#\#\#}P < 0.001$, $^{*}P < 0.05$, $^{**}P < 0.01$, $^{***}P < 0.001$ for each group of mice, n = 6).

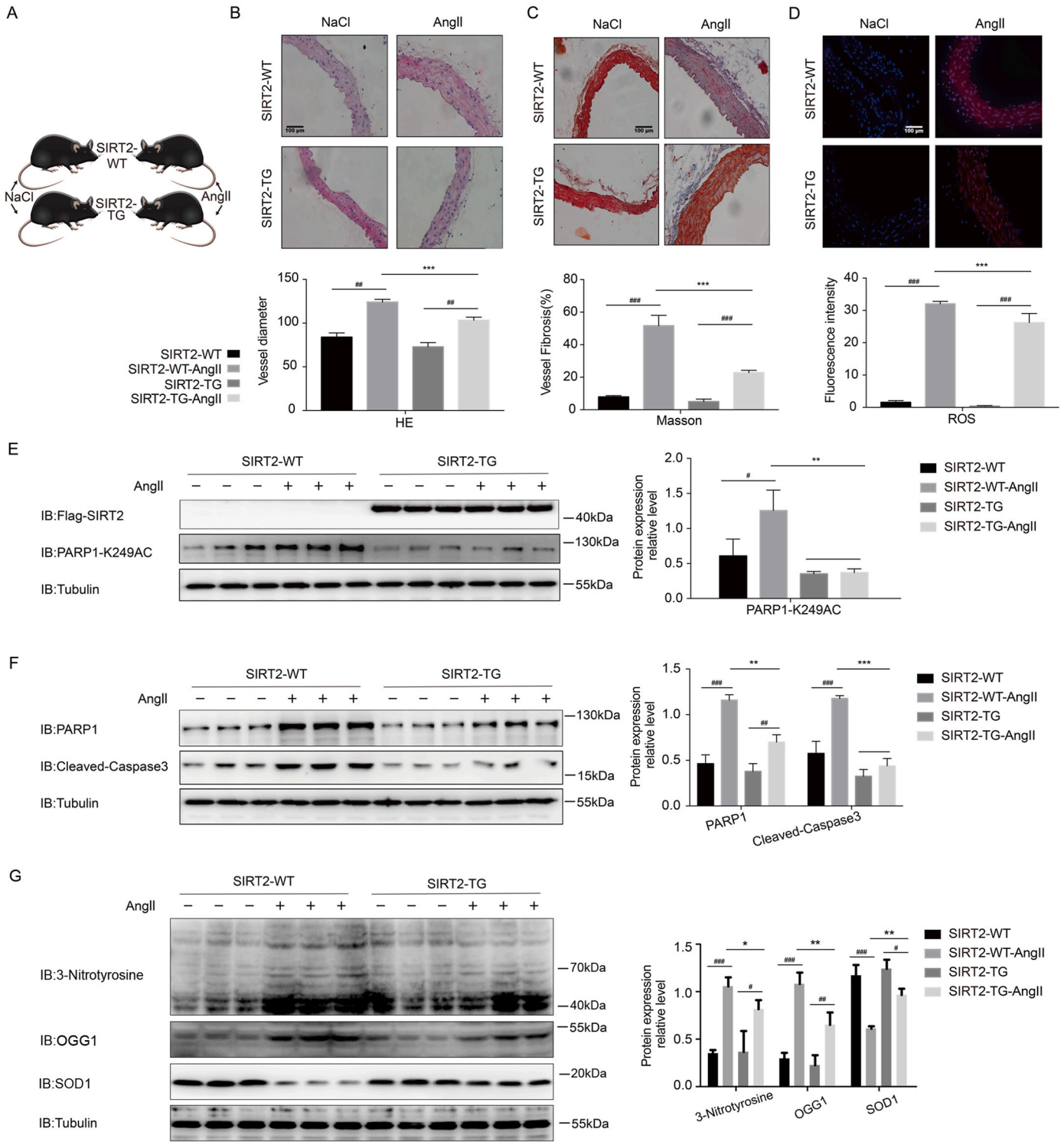

Fig. 6. SIRT2 overexpression significantly relieves Ang II-induced vascular injury and remodeling by decreasing PARP1-K249 acetylation and PARP1 levels in mice. (**A**) SIRT2-WT and SIRT2-TG mice were treated with either the control (NaCl) or Ang II (1.5 mg/kg/day) administered via a subcutaneously implanted osmotic minipump (Alzet, model 2002; 0.5 μl/h) for 14 days. Mice were euthanized by cervical dislocation after 14 days of treatment. (**B**) H&E staining, (**C**) Masson staining, and (**D**) DHE staining were performed to assess the degree of vascular thickening, vascular fibrosis, and vascular ROS production, respectively. Scale bar, 100 μm. Data are expressed as means ± SD ($^{\#\#}P < 0.01$, $^{\#\#\#}P < 0.001$, ***P < 0.001 for each group of mice, n = 6). (**E**) Total protein was obtained from the vascular tissue of SIRT2-WT and SIRT2-TG mice after infusion with either NaCl or Ang II for 14 days. Western blotting was performed to assess SIRT2 and PARP1-K249AC, or (**F**) PARP1 and Cleaved-Caspase3 expression levels as well as (**G**) 3-Nitrotyrosine, OGG1, and SOD1 expression levels. Quantification of western blot data is shown as the mean ± SD ($^{\#}P < 0.05$, $^{\#\#}P < 0.01$, $^{\#\#\#}P < 0.001$, *P < 0.05, **P < 0.01, ***P < 0.001 for each group of mice, n = 6).

subsequently impairs vascular function, stimulates inflammation and necrosis, and induces oxidative stress [20]. A previous study found that enhanced PARP1 activity causes vascular dysfunction, whereas reduced PARP1 activity overtly restores vascular functions [21]. Additionally, oxidative stress induces PARP1, thereby affecting Na^{+}-Ca^{2+} conversion, promoting Ca^{2+} ion influx, and ultimately promoting vascular dysfunction [22]. As described above, SIRT2 overexpression both in vivo and in vitro reduced PARP1-K249 acetylation and then reduced PARP1 levels and vascular damage, whereas SIRT2 knockdown had the opposite effects.

Probing the protective effect of SIRT2 on vascular damage revealed that SIRT2 deacetylated PARP1 and mobilized the ubiquitination of PARP1 by WWP2. The E3 ubiquitin ligase WWP2 mediates post-translational modification of target substrates by ubiquitination and participates in various cellular processes that include protein degradation, membrane protein transport, cell signaling, transcriptional regulation, and the cell cycle [6,7,23–26]. WWP2 was first observed in cancer studies. The related pathway WWP2-PTEN is a classic signaling pathway whose importance has been repeatedly confirmed in cancer research [24,25]. In recent years, a role of WWP2 has also been demonstrated in cardiovascular disease. Our previous study revealed that WWP2 regulates vascular injury and vascular remodeling after injury [6]. The present study showed that SIRT2 interacts with PARP1 at the PARP-A-helical domain, deacetylated PARP1, and then mobilized WWP2 to ubiquitinate PARP1 at the K249 site. Our previous findings also suggest that WWP2 indeed ubiquitinates PARP1 and promotes its degradation [7]. Additionally, the results of our cell and animal experiments indicated that SIRT2 negatively regulates PARP1. Therefore, the ubiquitination by WWP2 induced by SIRT2 degrades the vascular damage factor PARP1, thereby playing a role in resisting vascular damage and post-injury remodeling.

Future research should address the potential use of NAD boosters (like nicotinamide riboside or NMN) in order to keep cellular NAD levels high and thus enable SIRT2 to do its job and downregulate the level of PARP1, even though PARP1 is actively consuming cellular NAD. This aspect could lead to a future pharmacological/food-supplement-based strategy of breaking a biochemical “downward spiral” in the context of PARP1 mediated vascular injury.

In conclusion, through the discovery of the novel modification complex SIRT2-WWP2-PARP1 at mechanistic, cellular, and animal levels, this study provides new insights into treatment strategies for cardiovascular disease.

Declaration of competing interest

The authors have declared that no conflict of interest exists.

Acknowledgments

We thank Dr. Qunying Lei (Fudan University, Shanghai, China) for providing Flag-P300, Flag-CBP, and Myc-GCN5 plasmids, and Dr. Weiguo Zhu (Shenzhen University, Shenzhen, China) for providing Flag-PCAF.

Appendix A. Supplementary data

Supplementary data to this article can be found online at https://doi.org/10.1016/j.redox.2021.102141.

Author contributions

NJ.Z., Y.Z., YX.S., and L.C. conceived and designed the study; NJ.Z., Y.Z., BQ.W., and SJ.W. performed in vivo experiments; NJ.Z., Y.Z., SL.Y., SN.L., and JQ.X. conducted Co-IP and western blot analyses; Y.Z. carried out the immunohistochemistry; Co-IP and western blots were analyzed by Y.Z. and XY.H.; NJ.Z., Y.Z., JW.L., and XY.H. analyzed the data; NJ.Z. and Y.Z. wrote the initial manuscript and YX.S. and L.C. revised the manuscript.

Compliance with ethical standards

All animal experiments were approved by the Animal Subjects Committee of China Medical University and followed the Guide for the Care and Use of Laboratory Animals proposed by the US National Institutes of Health (NIH Publication No. 85-23, revised 1985).

Funding

This study was supported by National Natural Science Foundation of China (82171572, 82171571, 81970211, 81900355 and 81900372) and National Postdoctoral Innovative Talents Support Program (BX2021376).

References

[1] S.S. Virani, A. Alonso, E.J. Benjamin, M.S. Bittencourt, C.W. Callaway, A.P. Carson, et al., Heart disease and stroke statistics-2020 update: a report from the American heart association, Circulation 141 (9) (2020) e139–e596.
[2] P. Saharinen, L. Eklund, J. Miettinen, R. Wirkkala, A. Anisimov, M. Winderlich, et al., Angiopoietins assemble distinct Tie2 signalling complexes in endothelial cell-cell and cell-matrix contacts, Nat. Cell Biol. 10 (5) (2008) 527–537.
[3] P.C. Maisonpierre, C. Suri, P.F. Jones, S. Bartunkova, S.J. Wiegand, C. Radziejewski, et al., Angiopoietin-2, a natural antagonist for Tie2 that disrupts in vivo angiogenesis, Science 277 (5322) (1997) 55–60.
[4] S. Xu, P. Bai, P.J. Little, P. Liu, Poly(ADP-ribose) polymerase 1 (PARP1) in atherosclerosis: from molecular mechanisms to therapeutic implications, Med. Res. Rev. 34 (3) (2014) 644–675.
[5] R.J. Henning, M. Bourgeois, R.D. Harbison, Poly(ADP-ribose) polymerase (PARP) and PARP inhibitors: mechanisms of action and role in cardiovascular disorders, Cardiovasc. Toxicol. 18 (6) (2018) 493–506.
[6] N. Zhang, Y. Zhang, B. Wu, S. You, Y. Sun, Role of WW domain E3 ubiquitin protein ligase 2 in modulating ubiquitination and Degradation of Septin4 in oxidative stress endothelial injury, Redox Biol 30 (2020) 101419.
[7] N. Zhang, Y. Zhang, H. Qian, S. Wu, L. Cao, Y. Sun, Selective targeting of ubiquitination and degradation of PARP1 by E3 ubiquitin ligase WWP2 regulates isoproterenol-induced cardiac remodeling, Cell Death Differ. 27 (9) (2020) 2605–2619.
[8] L. Liu, L. Fan, M. Chan, M.J. Kraakman, J. Yang, Y. Fan, et al., PPARgamma deacetylation confers the antiatherogenic effect and improves endothelial function in Diabetes treatment, Diabetes 69 (8) (2020) 1793–1803.
[9] S. Basu, M. Barad, D. Yadav, A. Nandy, B. Mukherjee, J. Sarkar, et al., DBC1, p300, HDAC3, and Siah1 coordinately regulate ELL stability and function for expression of its target genes, Proc. Natl. Acad. Sci. U. S. A. 117 (12) (2020) 6509–6520.
[10] M. Zhang, W. Du, S. Acklin, S. Jin, F. Xia, SIRT2 protects peripheral neurons from cisplatin-induced injury by enhancing nucleotide excision repair, J. Clin. Invest. 130 (6) (2020) 2953–2965.
[11] S.H. Park, O. Ozden, G. Liu, H.Y. Song, Y. Zhu, Y. Yan, et al., SIRT2-Mediated deacetylation and tetramerization of pyruvate kinase directs glycolysis and tumor growth, Canc. Res. 76 (13) (2016) 3802–3812.
[12] B. Beirowski, J. Gustin, S.M. Armour, H. Yamamoto, A. Viader, B.J. North, et al., Sir-two-homolog 2 (Sirt2) modulates peripheral myelination through polarity protein Par-3/atypical protein kinase C (aPKC) signaling, Proc. Natl. Acad. Sci. U. S. A. 108 (43) (2011) E952–961.
[13] H.S. Kim, A. Vassilopoulos, R.H. Wang, T. Lahusen, Z. Xiao, X. Xu, et al., SIRT2 maintains genome integrity and suppresses tumorigenesis through regulating APC/C activity, Canc. Cell 20 (4) (2011) 487–499.
[14] Y.P. Wang, L.S. Zhou, Y.Z. Zhao, S.W. Wang, L.L. Chen, L.X. Liu, et al., Regulation of G6PD acetylation by SIRT2 and KAT9 modulates NADPH homeostasis and cell survival during oxidative stress, EMBO J. 33 (12) (2014) 1304–1320.

[15] X. Tang, X.F. Chen, N.Y. Wang, X.M. Wang, S.T. Liang, W. Zheng, et al., SIRT2 acts as a cardioprotective deacetylase in pathological cardiac hypertrophy, Circulation 136 (21) (2017) 2051–2067.
[16] M. Sarikhani, S. Mishra, S. Maity, C. Kotyada, D. Wolfgeher, M.P. Gupta, et al., SIRT2 deacetylase regulates the activity of GSK3 isoforms independent of inhibitory phosphorylation, Elife 7 (2018).
[17] A.C. Peterson, J.D. Russell, D.J. Bailey, M.S. Westphall, J.J. Coon, Parallel reaction monitoring for high resolution and high mass accuracy quantitative, targeted proteomics, Mol. Cell. Proteomics 11 (11) (2012) 1475–1488.
[18] J.B. Pillai, A. Isbatan, S. Imai, M.P. Gupta, Poly(ADP-ribose) polymerase-1-dependent cardiac myocyte cell death during heart failure is mediated by NAD+ depletion and reduced Sir2alpha deacetylase activity, J. Biol. Chem. 280 (52) (2005) 43121–43130.
[19] K. Yang, K.H. Lauritzen, M.B. Olsen, T.B. Dahl, T. Ranheim, M.S. Ahmed, et al., Low cellular NAD(+) compromises lipopolysaccharide-induced inflammatory responses via inhibiting TLR4 signal transduction in human monocytes, J. Immunol. 203 (6) (2019) 1598–1608.
[20] D.F. Dluzen, Y. Kim, P. Bastian, Y. Zhang, E. Lehrmann, K.G. Becker, et al., MicroRNAs modulate oxidative stress in hypertension through PARP-1 regulation, Oxid. Med. Cell Longev. (2017) 3984280, 2017.
[21] E.S. Liang, W.W. Bai, H. Wang, J.N. Zhang, F. Zhang, Y. Ma, et al., PARP-1 (Poly [ADP-Ribose] polymerase 1) inhibition protects from Ang II (angiotensin II)-Induced abdominal aortic aneurysm in mice, Hypertension 72 (5) (2018) 1189–1199.
[22] R. Alves-Lopes, K.B. Neves, A. Anagnostopoulou, F.J. Rios, S. Lacchini, A. C. Montezano, et al., Crosstalk between vascular redox and calcium signaling in hypertension involves TRPM2 (transient receptor potential melastatin 2) cation channel, Hypertension 75 (1) (2020) 139–149.
[23] S. Mokuda, R. Nakamichi, T. Matsuzaki, Y. Ito, T. Sato, K. Miyata, et al., Wwp2 maintains cartilage homeostasis through regulation of Adamts5, Nat. Commun. 10 (1) (2019) 2429.
[24] S. Maddika, S. Kavela, N. Rani, V.R. Palicharla, J.L. Pokorny, J.N. Sarkaria, et al., WWP2 is an E3 ubiquitin ligase for PTEN, Nat. Cell Biol. 13 (6) (2011) 728–733.
[25] J. Liu, L. Wan, J. Liu, Z. Yuan, J. Zhang, J. Guo, et al., Cdh1 inhibits WWP2-mediated ubiquitination of PTEN to suppress tumorigenesis in an APC-independent manner, Cell Discov. 2 (2016) 15044.
[26] P. Caron, T. Pankotai, W.W. Wiegant, M.A.X. Tollenaere, A. Furst, C. Bonhomme, et al., WWP2 ubiquitylates RNA polymerase II for DNA-PK-dependent transcription arrest and repair at DNA breaks, Genes Dev. 33 (11–12) (2019) 684–704.